

X-ray Performance of Back-Side Illuminated Type of Kyoto's
X-ray Astronomical SOI Pixel Sensor, XRPIX

MAKOTO ITOU¹, TAKESHI GO TSURU¹, TAKAAKI TANAKA¹, AYAKI TAKEDA¹,
HIDEAKI MATSUMURA¹, SHUNICHI OHMURA¹, SHINYA NAKASHIMA²,
YASUO ARAI³, KOJI MORI⁴, RYOTA TAKENAKA⁴, YUSUKE NISHIOKA⁴,
TAKAYOSHI KOHMURA⁵, KOKI TAMASAWA⁵, CRAIG TINDALL⁶

¹*Department of Physics, Graduate School of Science, Kyoto University,
Kitashirakawa Oiwake-cho, Sakyo-ku, Kyoto 606-8502, Japan*

²*Institute of Space and Astronautical Science (ISAS)/JAXA, 3-1-1 Yoshinodai,
Chuo-ku, Sagami-hara, Kanagawa 252-5210, Japan*

³*Institute of Particle and Nuclear Studies, High Energy Accelerator Research Org.,
KEK, 1-1 Oho, Tsukuba 305-0801, Japan*

⁴*Department of Applied Physics, Faculty of Engineering, University of Miyazaki,
1-1 Gakuen Kibana-dai Nishi, Miyazaki 889-2192, Japan*

⁵*Department of Physics, Faculty of Science and Technology,
Tokyo University of Science, 2641 Yamazaki, Noda, Chiba 278-8510, Japan*

⁶*Lawrence Berkeley National Laboratory, Berkeley, CA 94720, USA*

We have been developing X-ray SOI pixel Sensors, called “XRPIX”, for future X-ray astronomy satellites that enable us to observe in the wide energy band of 0.5–40 keV. Since XRPIXs have the circuitry layer with a thickness of about 8 μm in the front side of the sensor, it is impossible to detect low energy X-rays with a front-illuminated type. So, we have been developing back-illuminated type of XRPIX with a less 1 μm dead layer in the back-side, which enables the sensitivity to reach 0.5 keV. We produced two types of back-side illuminated (BI) XRPIXs, one of which is produced in “Pizza process” which LBNL developed and the other is processed in the ion implantation and laser annealing. We irradiated both of the BI-XRPIXs with soft X-ray and investigate soft X-ray performance of them. We report results from soft X-ray evaluation test of the device.

PRESENTED AT

International Workshop on SOI Pixel Detector
(SOIPIX2015)
Tohoku University, Sendai, Japan, 3-6, June, 2015

1 Introduction

Charge-coupled devices (CCDs) are standard imaging spectrometers widely used in modern X-ray astronomy. They have a good performance of spectroscopy and imaging because of their small pixel sizes ($20\ \mu\text{m} \sim 30\ \mu\text{m}$) and the Fano-factor limitation on the energy-resolution ($\sim 130\ \text{eV}$ in FWHM at $6\ \text{keV}$) [1]-[3]. However, CCDs suffer from the problem such as a high non-X-ray (NXB) background above $10\ \text{keV}$ induced by the interactions with cosmic-rays in orbit. One of ways of solving this problem is adopting an anti-coincident technique with surrounding scintillators as active shields[4][5]. On the other hand, CCDs do not have a good time-resolution which is enough to adopt this technique. Thus, we have been developing X-ray SOI pixel sensors, called “XRPIX”, which overcome the limitations of CCDs, in order to realize wide-band X-ray imaging spectroscopies for the future X-ray astronomy[6]. XRPIXs enable us to observe with a high time-resolution of $\sim 10\ \mu\text{sec}$, which allows us to employ anti-coincidence shields and reject NXB.

XRPIXs are the monolithic active pixel sensors, which are processed with the silicon-on-insulator (SOI) CMOS technology[7]. As Figure 1 shows, an XRPIX consists of three layers: a circuit with low-resistivity silicon ($\sim 8\ \mu\text{m}$), a sensor with high-resistivity silicon, and SiO_2 insulator between two.

In order to detect X-rays with the energies above $\sim 10\ \text{keV}$, we need to develop the XRPIX with the Si thick sensor-layer. We need to use the back-side of the XRPIX (back-illumination, BI) as an entrance face for incident X-rays because a circuitry layer on the front-side of it prevents us from detecting low-energy X-rays below $1\ \text{keV}$. A dead layer on the X-ray incident surface should ideally be as thin as possible to achieve a high sensitivity to low-energy X-rays. Thus, the fully-depleted BI-type of XRPIX with a thin dead layer is required to realize the wide bandpass performance. In this paper, we report the X-ray performance of the first BI-types of XRPIXs, “XRPIX-FZ-LA” and “XRPIX-CZ-PZ”.

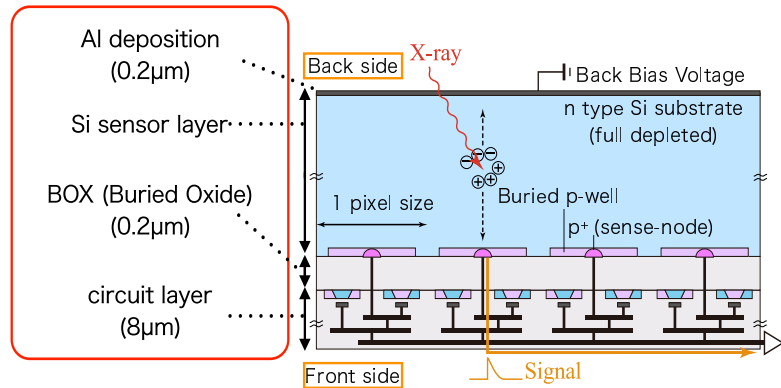


Figure 1: The cross-sectional view of XRPIX.

2 Experimental Setup

We irradiated XRPIX with Ti-K and Cu-K. Ti-K (4.51 keV) and Cu-K (8.04 keV) lines have attenuation lengths of $13.1 \mu\text{m}$ and $67.3 \mu\text{m}$, respectively. Figure 2 shows the schematic of the experimental setup in the vacuum chamber. XRPIX is connected to the cold head and cooled by Iwatani pulse tube cooler (Iwatani CryoMini P003) to cool the XRPIX to -50°C . We use a readout system consisting of a sub board with which an XRPIX is equipped, and a SEABAS (Soi EvAluation BoARd with Sitcp) board. Details of the readout system are reported in [10].

Before the performance evaluation of XRPIXs, we observed the spectra and absolute flux of the Ti-K and Cu-K lines with a silicon drift detector (SDD: Amptek XR-100). Figure 3 shows the spectrum of illuminated X-ray obtained with the SDD. Ti-K lines at 4.51 keV and 4.93 keV and Cu-K lines at 8.04 keV and 8.90 keV are seen. We obtained absolute fluxes of the lines at the position of the XRPIX, referring to the quantum efficiency and the collimator size of the SDD given in the Amptek website[11], and correcting the difference in the distances from the secondary target to the XRPIX and SDD. The errors in the absolute fluxes are dominated by the systematic error of the collimator area of the SDD ($\pm 10\%$).

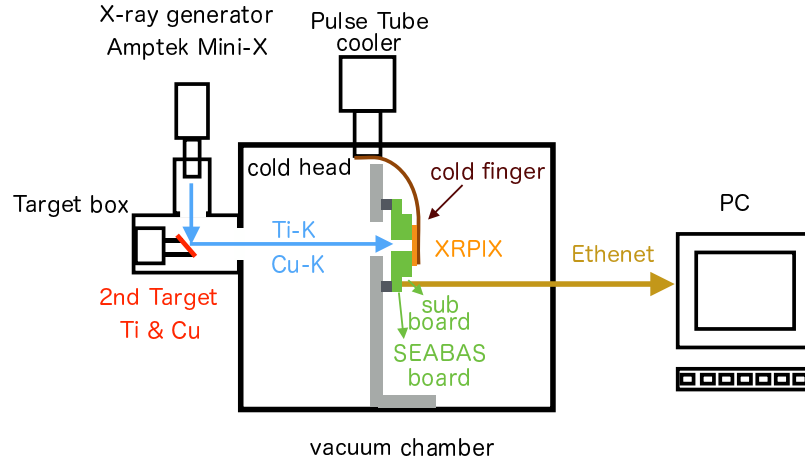


Figure 2: The picture of the experimental setup.

3 XRPIX-FZ-LA

3.1 Device Discription

We produced two BI-XRPIXs, named “XRPIX-FZ-LA” and “XRPIX-FZ-PZ”. So, we introduce specifications of them, which are summarized in table 1. We used the $0.2\text{-}\mu\text{m}$ CMOS fully-depleted SOI CMOS Pixel process provided by Lapis Semiconductor

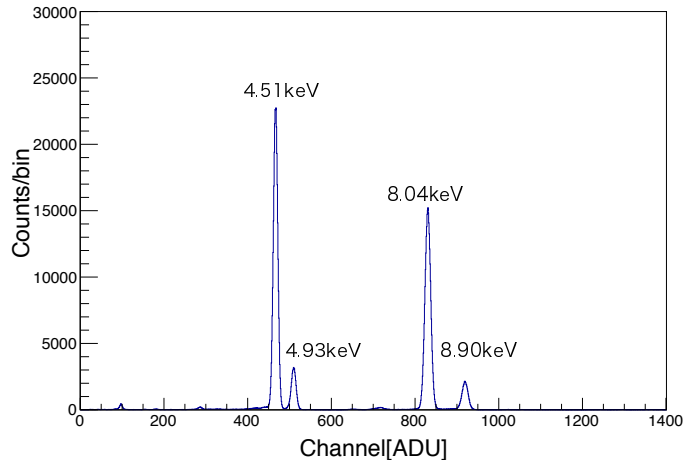


Figure 3: The spectrum obtained by SDD.

Co. Ltd.. Two BI-XRPIXs are different in terms of the resistivity in the Si sensor-layers. One is the Floating Zone (FZ) device with nominal resistivity is $\sim 4 \text{ k}\Omega\cdot\text{cm}$, and the other one is the Czochralski (CZ) device with nominal resistivity is $\sim 1.2 \text{ k}\Omega\cdot\text{cm}$. The XRPIX-FZ-LA has the FZ-type Si sensor-layer with the thickness of $500 \text{ }\mu\text{m}$. On the back-side of a sensor layer, chemical etching, ion implantation, laser annealing, and vapor-deposition of aluminum (200 nm) for optical blocking are processed.

Table 1: Specifications of XRPIX-FZ-LA and -CZ-PZ

	XRPIX2b-FZ-LA	XRPIX2b-CZ-PZ
Pixel size ($\mu\text{m} \times \mu\text{m}$)	30×30	
Format (pixels)	152×152	
Wafer type	Floating Zone	Czochralski
Nominal Resistivity ($\text{k}\Omega\cdot\text{cm}$)	~ 4	~ 1.2
Sensor layer (μm)	500	62
Back-side process	ion implantation, laser annealing	Pizza process
Al deposition	$0.2 \text{ }\mu\text{m}$	none

3.2 Experiments and Results

With the XRPIX-FZ-LA, we obtained spectra and the flux of Ti-K and Cu-K with back-bias voltages (V_{bb}) from 140 V to 300 V . The chip was cooled to $-40 \text{ }^\circ\text{C} \sim -30 \text{ }^\circ\text{C}$ at the degree of vacuum lower than 10^{-5} Torr . We performed a frame-by-frame

readout, where all the pixels are sequentially read out after a 1 ms exposure. The total exposure time is 300 s, respectively. The details of the readout sequence is reported in [12]. In order to classify charge sharing events, we used the methods described in [12] and [13]. We picked up a pixel whose pulse height exceeds a predefined threshold called event threshold. Then, we checked pulse height of adjacent 8 pixels whether they exceed a split threshold and classified each X-ray event into four event types of “single pixel”, “double pixel”, “triple pixel”, and “other”. In this analysis, the readout noise is 59 e^- , the event threshold is 2.4 keV, and the split threshold is 0.5 keV.

Figure 4 shows spectra obtained by XRPIX-FZ-LA with back bias voltages from 160V to 300V. Figure 5 and 6 shows the quantum efficiency of each grades separately as a function of the applied back-bias voltage. These figures indicate that count rates of Ti-K and Cu-K increase. When we changed back V_{bb} from 160V to 300V, the ratio of Ti-K counts becomes 11.11. Similarly, one of Cu-K counts becomes 1.58. The growth rate of counts is clearly different between Ti-K and Cu-K. From this result, we understand the depletion layer in the Si sensor-layer spreads from the front-side of face to the back-side of one. The QE with the sum of four grades become constant at $V_{bb} \geq 220\text{V}$. The QE of Cu-K line is consistent with the expected value for absorption in the Si sensor-layer with the thickness of $500\text{ }\mu\text{m}$. This results suggest the Si sensor-layer gets fully depleted at $\sim 220\text{ V}$.

Figure 7 shows the thickness of the dead layer which we estimated from the QEs of Ti-K and Cu-K as a function of V_{bb} . Ti-K line’s attenuation length is shorter than Cu-K’s one. So, the dead layer at $V_{bb} \geq 220\text{ V}$ is also obtained from the QEs of Ti-K in order to estimate it accurately. Before the Si sensor-layer gets fully depleted, the dead layer is thicker. So, we estimated the thickness of the dead layer at $V_{bb} < 220\text{ V}$ from the QE of Cu-K. From these results, the thickness of the dead layer is $1.9 \pm 0.9\text{ }\mu\text{m}$ which includes the Al deposition layer of $0.2\text{ }\mu\text{m}$ thick.

According to the above, XRPIX-FZ-LA is a full depleted device, but its dead layer is not satisfied with the requirement of $1\text{ }\mu\text{m}$. In order to achieve the higher sensitivity to low-energy X-rays, we need to improve the device.

We discuss whether the thickness of the Si sensor-layer is adequate to detect low-energy X-rays. The sensor-layer with thickness of $500\text{ }\mu\text{m}$ is thick enough to observe in the high energy X-ray band. On the other hand, the single pixel events don’t have a small proportion of the sum of X-ray events due to the thick sensor-layer. In other words, the charge clouds expand along the electric flux line, which are shared by multi pixels. This phenomenon is seen in Figure 5 and 6. Since charge collection efficiency is better as higher V_{bb} is applied, the charge of Ti-K is smaller, and the triple and other pixel events decrease. According to Figure 5 and 6, the single pixel event is about $10 \sim 20\%$ of the charge. The large number of multi pixel events make the readout noise increase effectively. In order to achieve the good performance of spectroscopy enough to observe low-energy X-rays and estimate the thickness of dead

layer, the sensor-layer is thinner than $500\text{ }\mu\text{m}$. So, we developed the device with the thinner Si sensor-layer which is produced by new back-side process.

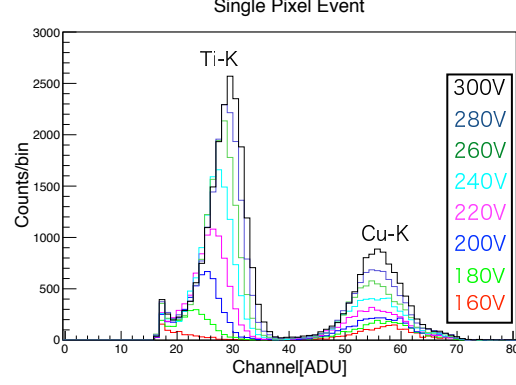


Figure 4: The spectra of single pixel events obtained for various back bias voltages with XRPIX-FZ-LA.

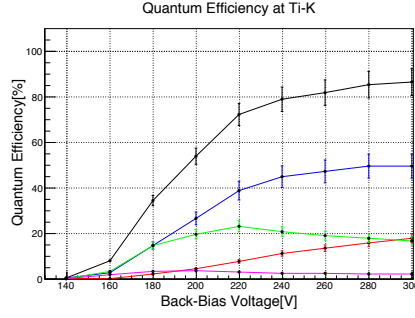


Figure 5: Quantum efficiency of each grade with XRPIX-FZ-LA at the energy of Ti-K X-rays as a function of V_{bb}

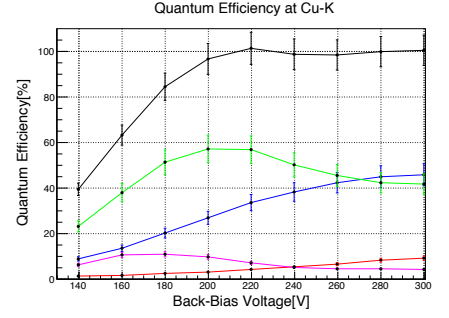


Figure 6: Same as Figure 5 but at the energy of Cu-K X-rays.

4 XRPIX-CZ-PZ

We fabricated the devices, “XRPIX2b-CZ-PZ”, which has a thin Si sensor-layer of $62\text{ }\mu\text{m}$ thick and the back-side treated with the Pizza process, developed by LBNL[8]. The specifications of the device are given in Table 1. Pizza process” is the way of processing the back-side widow and goes through the following procedure. First, the Si wafer is back-thinned to $70\text{ }\mu\text{m}$ by using grinding technique. Second, a thin

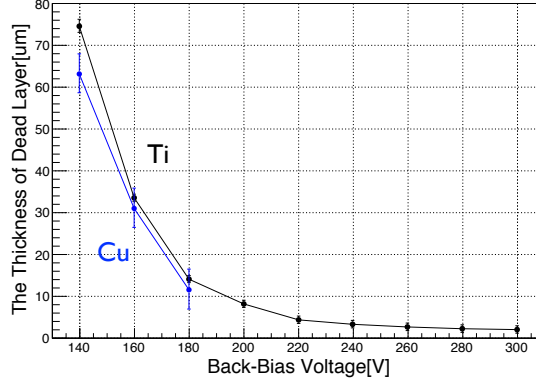


Figure 7: The Thickness of Dead Layer@XRPIX-FZ-LA

phosphor layer is made in the wafer by ion-implantation at $-160\text{ }^{\circ}\text{C}$. Finally, it is annealed at $500\text{ }^{\circ}\text{C}$ for 10 min like baking a pizza. The details of the process is give in [8].

Figure 8 shows that the spectra obtained by XRPIX-CZ-PZ with back bias voltages of $20\text{V} \sim 70\text{V}$. In this analysis, the readout noise is 44 e^- , and we use the same event and split threshold as XRPIX-FZ-LA. We can see Cu- $\text{K}\alpha$ and Cu- $\text{K}\beta$ separated from Cu-K line. The spectra with different back bias voltages are completely different. As higher back bias voltage is applied, the event of Ti-K increases exactly. Figure 9 and 10 show the QE of each grades as a function of the V_{bb} . According to these figures, the ratio of Ti-K counts becomes 2.24 when we change back bias voltage from 20V to 70V . Similarly, one of Cu-K counts becomes 1.06. From this result, we can understand the dead layer is thinner as the depletion region spreads. The QE with the sum of four grades become constant at $V_{bb} \geq 40\text{V}$. The QE of Cu-K line is consistent with the expected value for absorption in the Si sensor-layer with the thickness of $62\text{ }\mu\text{m}$. This results suggest the Si sensor-layer gets fully depleted at $\sim 40\text{ V}$. The QE of Ti-K increases as the back bias voltage that is higher and becomes almost constant when $\geq 40\text{V}$.

Figure 11 shows the thickness of the dead layer which we estimated from the QEs of Ti-K and Cu-K as a function of V_{bb} . From this results, the thickness of dead layer is $1.2 \pm 1.1\text{ }\mu\text{m}$. The thickness of dead layer nearly satisfies the requirement for future X-ray satellite. This large error suggests that the attenuation length of Ti-K is long enough to estimate the thickness of the dead layer. So, we need to estimate the thickness of the dead layer with a fluorescent X-ray with the shorter attenuation length than the one of Ti-K. We have developed the

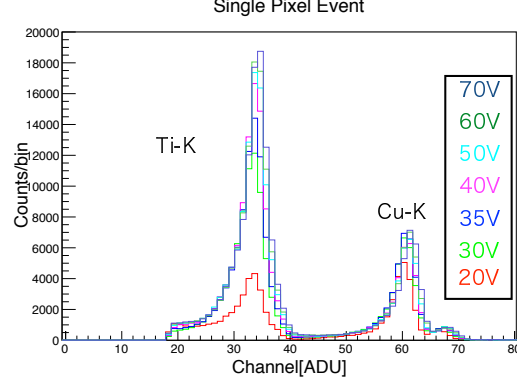


Figure 8: The spectrum obtained by XRPIX2b-CZ-Pizza

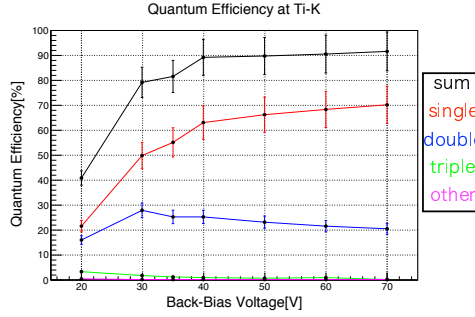


Figure 9: Quantum efficiency of each grade with XRPIX-CZ-PZ at the energy of Ti-K X-rays as a function of V_{bb}

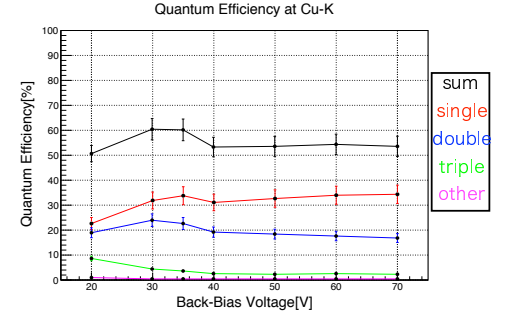


Figure 10: Same as Figure 9 but at the energy of Cu-K X-rays.

5 Summary and Future Plan

We have been developing back-illuminated types of XRPIXs in order to have good sensitivity down to 0.5 keV for future satellite. We evaluate the thickness of the performance for low-energy X-rays and dead layer of XRPIX-FZ-LA and XRPIX-CZ-PZ. The dead layer thickness of XRPIX-FZ-LA is $1.9 \pm 0.9 \mu\text{m}$, and the one of XRPIX-CZ-PZ is $1.2 \pm 1.1 \mu\text{m}$. These result suggest the thickness of the dead layer nearly satisfies the requirement for a future X-ray satellite. In the next experiments, we will evaluate the dead layer thickness and Charge-Collection-Efficiency (CCE) etc. by using lower energy X-rays such as Cl-K and Al-K line.

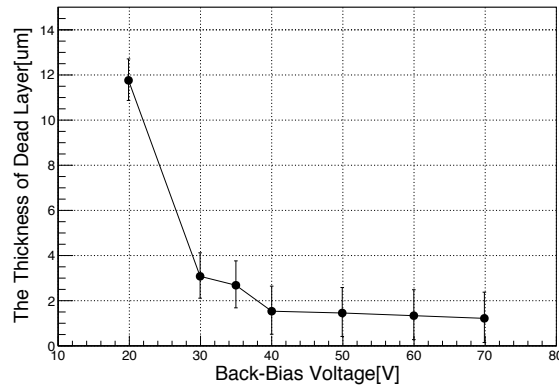


Figure 11: The Thickness of Dead Layer@XRPIX-CZ-PZ

References

- [1] G.P. Garmire et al., Advanced CCD imaging spectrometer (ACIS) instrument on the Chandra X-Ray Observatory, Proc. SPIE 4851 28 (2003).
- [2] M. J. L. Turner et al., The European Photon Imaging Camera on XMM-Newton: The MOS cameras, Astronomy & Astrophysics, 365 L27 (2001).
- [3] K. Koyama et al., X-Ray Imaging Spectrometers (XIS) on Board Suzaku, Publication of the Astronomical Society of Japan, 59 S22 (2007).
- [4] T. Takahashi et al., Hard X-Ray Detector (HXD) on Board Suzaku, Publication of Astronomical Society of Japan, 59 (2007) S35.
- [5] T. Anada, T. Dotani, M. Ozaki and H. Murakami, Instrumental background of the X-ray CCD camera in space: its dependence on the configuration parameters of CCD, Proc. SPIE 7011 (2008) 70113X.
- [6] T.G.Tsuru et al., Development and Performance of Kyoto's X-ray Astronomical SOI pixel (SOIPIX) sensor, SPIE, 9144 (2014) 914412.
- [7] Y. Arai et al., Development of SOI Pixel Process Technology, Nuclear Instruments and Methods in Physics Research Section A, 636 S31 (2011).
- [8] M. Battaglia et al., Characterisation of a Thin Fully Depleted SOI Pixel Sensor with Soft X-ray Radiation, Nuclear Instruments and Methods in Physics Research Section A, 674 51-54 (2012).
- [9] A.Takeda et al., Improvement of spectroscopic performance using a charge-sensitive amplifier circuit for an X-ray astronomical SOI pixel detector, Journal of Instrumentation, 10 C06005 (2015).

- [10] T. Uchida, Hardware-Based TCP Processor for Gigabit Ethernet, IEEE Transactions on Nuclear Science, 55 3 1631 (2008).
- [11] The quantum efficiency of the Silicon Drift Detector (Amptek XR-100), <http://www.amptek.com/products/xr-100sdd-silicon-drift-detector/>
- [12] Ryu et al., First Performance Evaluation of an X-Ray SOI Pixel Sensor for Imaging Spectroscopy and Intra-Pixel Trigger, IEEE Transactions on Nuclear Science, 58 2528 (2011).
- [13] Nakashima et al., Progress in Development of Monolithic Active Pixel Detector for X-ray Astronomy with SOI CMOS Technology, Physics Procedia, 37 (2012) 1373.